

DOI: 10.1002/adfm.200600267

# Ultrafast Spectroscopic Study of Photoinduced Electron Transfer in an Oligo(thienylenevinylene):Fullerene Composite\*\*

By In-Wook Hwang, Qing-Hua Xu, Cesare Soci, Baoquan Chen, Alex K.-Y. Jen, Daniel Moses,\* and Alan J. Heeger

Photoinduced electron transfer and competing processes have been studied in composites of an oligo(thienylenevinylene) (OTV), comprised of ten dibuthoxyl-thiophene units separated by vinylene units, and a C<sub>60</sub> derivative, [6,6]-phenyl-C<sub>61</sub> butyric acid methyl ester (PCBM), by using femtosecond transient absorption spectroscopy and sub-nanosecond transient photoconductivity. We find that in OTV:PCBM the photoexcitations decay primarily via intrachain relaxation rather than photoinduced electron transfer from OTV to PCBM. The electron-transfer process requires ca. 14 ps; larger by more than two orders of magnitude than the required time observed in conjugated-polymer:C<sub>60</sub> composites, and also larger than the 0.6 ps singlet-state lifetime in OTV. These observations indicate that the quantum efficiency for photoinduced electron transfer in OTV:PCBM is less than 5%.

## 1. Introduction

Ultrafast photoinduced electron transfer from semiconducting polymers to fullerenes (C<sub>60</sub>) has been reported.<sup>[1–3]</sup> Because the electron transfer rate ( $> 10^{13} \text{ s}^{-1}$ ) is several orders of magnitude larger than any competing decay process, the quantum efficiency of the electron-transfer process is close to unity.<sup>[2–5]</sup> The ultrafast electron transfer and the associated high quantum efficiency provide a pathway for the development of high-efficiency photodetectors and photovoltaic cells fabricated from semiconducting polymers.

In general, there has been good progress toward efficient polymer-based solar cells, and efficiencies of approximately

5% have been demonstrated.<sup>[6,7]</sup> Improvements beyond 5% will require the identification of semiconducting polymers with absorption spectra that are well-matched to the solar radiation spectrum. Poly(thienylenevinylene) (PTV) has a relatively small energy gap ( $E_g$ ) of ca. 1.6 eV, and a good hole mobility ( $\mu_h$ ) of ca.  $0.22 \text{ cm}^2 \text{ V}^{-1} \text{ s}^{-1}$ ,<sup>[8]</sup> features that are promising for high-efficiency, polymer-based solar cells.<sup>[9]</sup>

Here, we focus on the photoexcitation relaxation dynamics in an oligo(thienylenevinylene) (OTV), comprised of ten dibuthoxyl-thiophene units separated by vinylene units (shown in Scheme 1), and in composites of OTV with a C<sub>60</sub> derivative, [6,6]-phenyl-C<sub>61</sub> butyric acid methyl ester (PCBM), by using time-resolved spectroscopic methods. We find that in OTV:PCBM, the photoexcitations decay principally via intrachain relaxation rather than electron transfer from OTV to PCBM, as commonly seen in composites of C<sub>60</sub> with conjugated polymers such as the poly(phenylenevinylene)s (PPVs) and poly(thiophene)s (PTs). In OTV:PCBM, electron transfer occurs after approximately 14 ps. This value is larger by more than two orders of magnitude than values typically observed in conjugated-polymer:C<sub>60</sub> composites, and significantly longer than the singlet-state lifetime in OTV (0.6 ps). These observations indicate that the quantum efficiency for photoinduced electron transfer is less than 5% in OTV:PCBM. Initially, the photoconductivity and photoinduced absorption signals from the separated charge carriers decay exponentially with time, with a constant decay rate of approximately 0.8 ns, followed in time by an almost constant response in the nanosecond time regime.

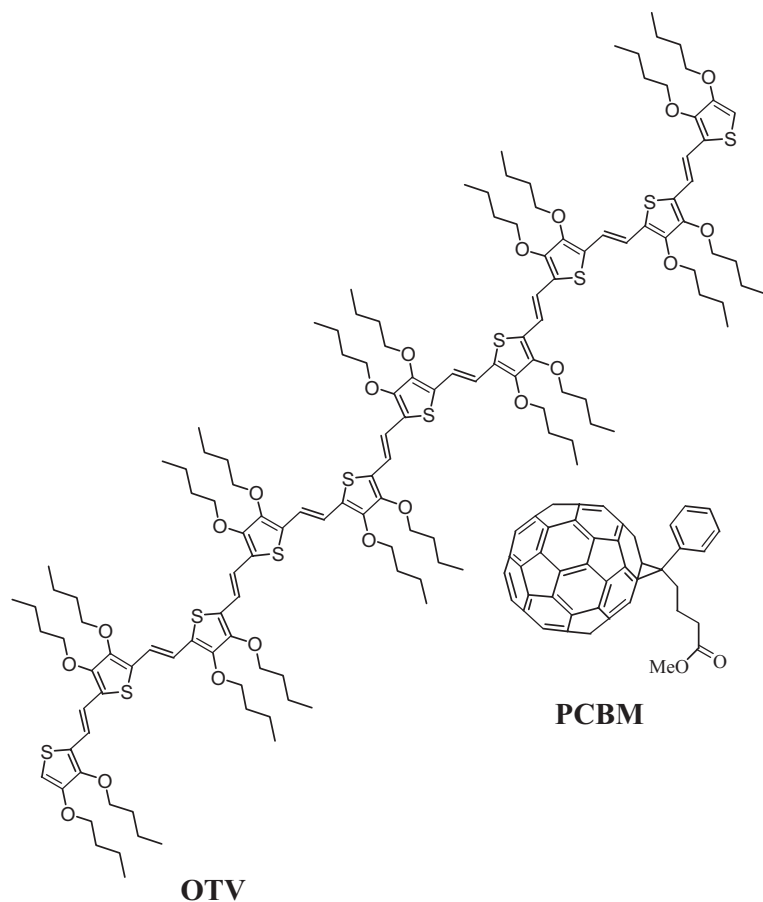
When probing at 700 nm, we detect a coherent modulation of the photobleaching signal in OTV, which arises from the generation and propagation of acoustic waves in the OTV film. The period of this acoustic wave modulation of the PIA signal allows us to determine the sound velocity in this system as  $1.6 \times 10^5 \text{ cm s}^{-1}$ .

[\*] Dr. D. Moses, Dr. I.-W. Hwang, Dr. Q.-H. Xu,<sup>[†]</sup> Dr. C. Soci, Prof. A. J. Heeger  
Center for Polymers and Organic Solids  
University of California Santa Barbara  
Santa Barbara, CA 93106-5090 (USA)  
E-mail: moses@physics.ucsb.edu

B. Chen, Prof. A. K.-Y. Jen  
Department of Materials Science and Engineering  
University of Washington  
Box 352120, Seattle, WA 98195-2120 (USA)

[†] Current address: Department of Chemistry, National University of Singapore, 3 Science Drive, Singapore 117543, Singapore.

[\*\*] Research at UCSB was funded by a grant from the National Science Foundation (NSF-DMR 0602280), support from the Air Force Office of Scientific Research through the MURI Center ("Smart Skins"), Charles Lee, Program Officer, and the Korea Research Foundation (KRF-2005-M01-2004-000-20037-0-C00179). Research at the University of Washington was supported by Air Force Office of Scientific Research through the MURI Center ("Smart Skins"), Charles Lee, Program Officer. We thank Jonathan Yuen for his technical assistance with evaluating the film thickness. Supporting Information is available online from Wiley InterScience or from the author.



**Scheme 1.** Molecular structures of oligo(thienylenevinylene) (OTV) and [6,6]-phenyl- $C_{61}$  butyric acid methyl ester (PCBM). A 1:1 weight ratio was used for the composite.

## 2. Results

Figure 1 shows the steady-state absorption spectra of OTV and OTV:PCBM films as well as that of PCBM in solution. The OTV film does not show a detectable fluorescence, in agreement with other reports.<sup>[10,11]</sup> The data exhibit a broad absorption profile, ranging from the UV to ca. 750 nm, and well-defined vibronic side bands in the 600–700 nm region. The onset of the absorption energy implies a rather small energy gap between the highest occupied molecular orbital (HOMO) and the lowest unoccupied molecular orbital (LUMO) in OTV. The absorption spectrum of the OTV:PCBM composite is a superposition of the two individual components (i.e., the absorption spectra of OTV and PCBM), implying phase separation with little or no change in the electronic structure. PCBM shows absorption bands centered at 340 and 530 nm.

The results of steady-state and time-resolved photoconductivity (PC) measurements are displayed in Figure 2. The steady-state PC of OTV:PCBM shows a broad action spectrum (shown in the inset of Fig. 2) similar to the absorption spectrum of the film (Fig. 1). The transient PC waveform for OTV exhibits an extremely rapid decay, faster than the temporal res-

olution of the measuring system, which indicates fast charge recombination and/or trapping processes occurring at timescales  $t < 100$  ps. The transient PC for OTV:PCBM exhibits a similar initial fast decay ( $t < 100$  ps) followed by a long-lived tail. The long-lived tail consists of two components, one with a time constant of 0.85 ns, followed by an almost constant photoconductive response in the nanosecond time regime. This long-lived PC arises from the metastable charge separation in the bulk heterojunction material.<sup>[2]</sup>

The transient absorption (TA) spectra are shown in Figure 3. The OTV spectrum exhibits two photo-bleaching (PB) bands at 520 and 680 nm and two photoinduced absorption (PIA) bands at 750 and 1000 nm (Fig. 3, upper panel). For most of the probe wavelengths (with the exception of the one at ca. 700 nm) the TA signal decays with a short time constant of ca. 1 ps, while the one probed at 700 nm indicates a relatively long-lived PB band. The data for OTV:PCBM composite show different TA characteristics than those found for OTV (Fig. 3, lower panel), where relatively long-lived PB bands appear at 400–700 nm and a long-lived PIA band is observed at 950 nm. The long-lived PB bands at 400–700 nm indicate delayed electron–hole recombination dynamics, resulting from electron transfer from OTV to PCBM. The long-lived PIA band centered at 950 nm arises from the photoinduced absorption originating from the charge-transferred state; this band is similar to the charge-transfer band observed in the near infrared regime in the PT: $C_{60}$  system.<sup>[2,12]</sup>

To clarify the excited-state relaxation dynamics in pristine OTV, the TA decay profiles were probed at several wavelengths (left panels in Fig. 4). The parameters inserted in each panel of Figure 4 represent the results for the rise and

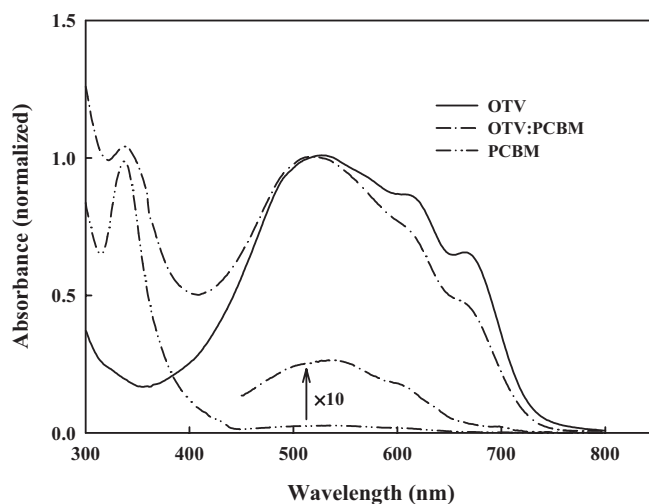


**Figure 1.** Steady-state absorption spectra of OTV, OTV:PCBM (1:1) films, and that of PCBM in chlorobenzene.

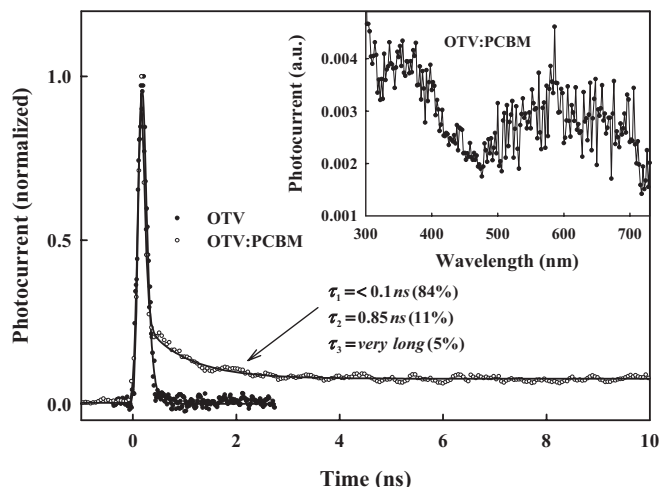


**Figure 2.** Transient photoconductivities of OTV and OTV:PCBM (1:1) films. The inset shows the steady-state photoconductivity spectrum of OTV:PCBM. The applied bias voltage was 500 V. The pump intensity was  $200 \mu\text{J cm}^{-2}$ .

decay times as well as the relative amplitudes, indicated in percentage of their sum of each component obtained from fitting the data to either single or double exponential forms deconvolved from the excitation pulse profile. Except for the data obtained at 700 nm, the TA decay is well-described by the two components characterized by time constants of 0.6 and 1.6 ps. When probed at 700 nm and 750 nm, we found the rise time to be longer than the temporal resolution of the measuring system. Interestingly, the decay of the TA signal at 700 nm is significantly longer-lived and oscillating (bottom left panel in Fig. 4). As will be discussed in the following, these oscillations manifest a coherent propagation of acoustic phonons across the OTV film.

Compared to the OTV, the OTV:PCBM composite shows different signal-decay dynamics (right panels in Fig. 4). These data were fitted to a sum of two or three exponential terms. When probed at 600, 750, and 1000 nm, the initial two decay time constants are similar to those observed in OTV, but in general a characteristic longer-lived tail is evident in OTV:PCBM at all wavelengths. When probing at 700 nm, the signal rise and decay profiles are different from those of OTV; the signal appears after approximately 14 ps and decays with two components, one with a time constant of ca. 0.8 ns followed by an almost constant TA response in the nanosecond time regime. The long-lived TA tails found in the OTV:PCBM composite reflect the long-lived separated carriers that result from the electron transfer reaction from OTV to PCBM.

A more complete picture of the electron-transfer process in the OTV:PCBM composite was obtained from measurements of the TA at longer times (Fig. 5). The most important observation is that the electron-transfer rate in this system is significantly slower than typically found in conjugated-polymer:C<sub>60</sub> composites, for example, approximately 45 fs in PPV:PCBM.<sup>[4]</sup> This can be seen from the PIA data for OTV:PCBM at 950 nm, shown in Figure 5b. The fast initial decay is consistent

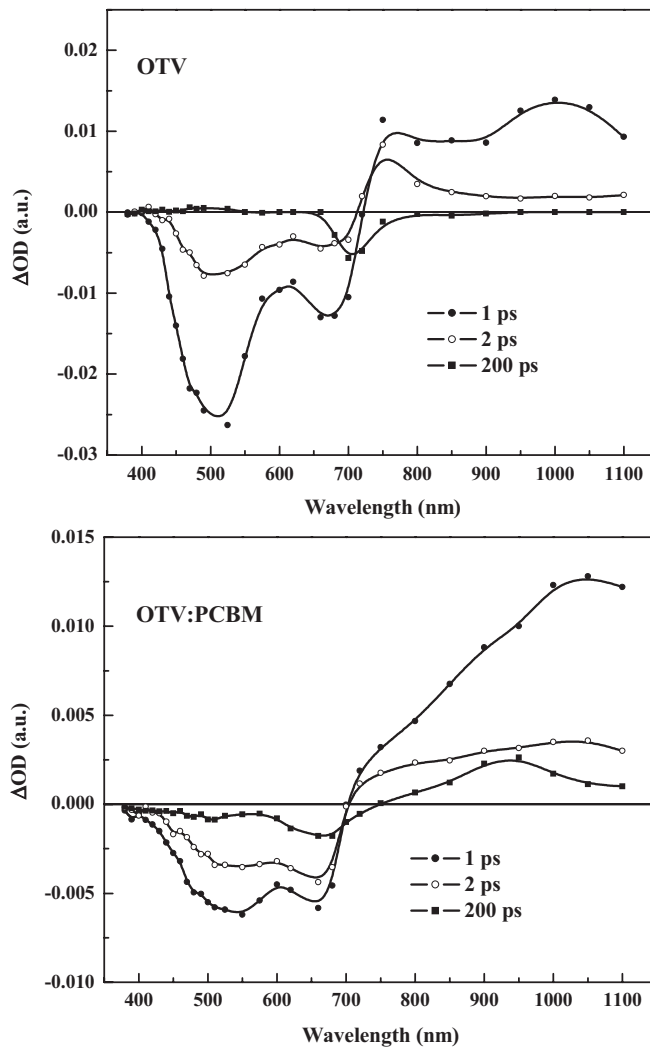


**Figure 3.** Transient absorption spectra of OTV (upper) and OTV:PCBM (1:1) (lower) films. The spectra were measured at the delay times 1, 2, and 200 ps. The pump wavelength was 650 nm.

with the temporal evolution of the excitations in OTV (see  $\lambda_{\text{probe}} = 1000 \text{ nm}$  data shown in Fig. 4), and thus can be assigned to the relaxation of the neutral excitations in OTV. This initial response is followed by an increase in the PIA signal (with a characteristic time constant of 14 ps) that eventually slowly decays. We assign the latter to the photoinduced absorption by the charge carriers (e.g., the polaron absorption) as the electron transfer process generates an increasing density of electrons and holes on the PBCM and OTV sites, respectively. Eventually, this PIA signal decays as the carriers recombine, with the time constants indicated in the inset of Figure 5b. The long-lived charge-transfer state seen in Figure 5b is consistent with the long-lived transient photocurrent depicted in Figure 2. Confirmation of these assignments can be inferred from Figure 5a, where the PB signal probed at 600 nm exhibits a fast initial decay followed in time by a longer-lived tail. The fast initial decay is similar to that of the neutral excitations in OTV, whereas the longer-lived tail decaying with a time constant of

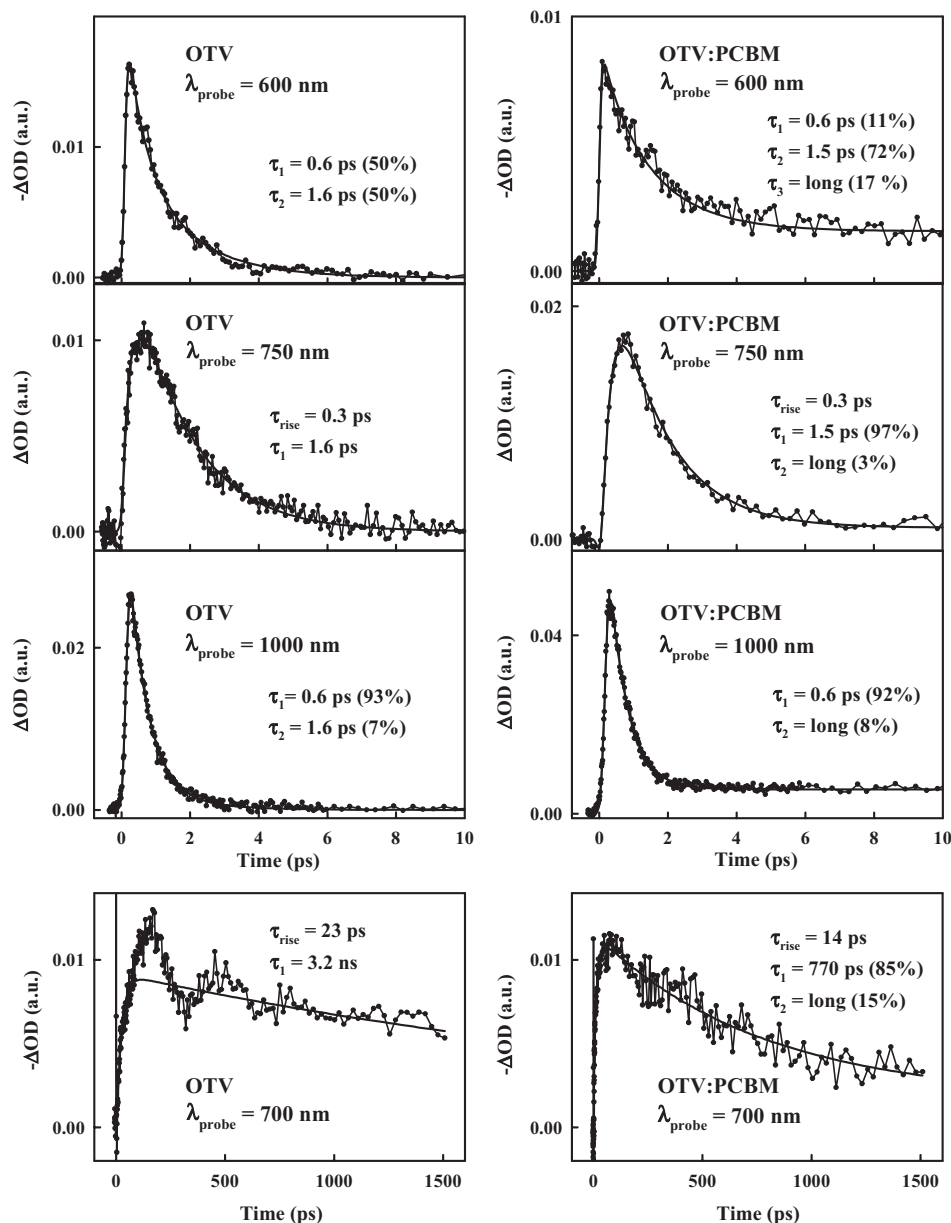


**Figure 4.** Transient absorption decay profiles of OTV (left panels) and OTV:PCBM (1:1) (right panels) films: the decay dynamics were probed at 600, 750, and 1000 nm using a time-window of 10 ps, and at 700 nm using a time-window of 1500 ps. The fitted decay parameters are inserted in each panel. The pump wavelength and intensity were 650 nm and 200  $\mu\text{J cm}^{-2}$ . There was no high pump intensity effect on the measured decay profiles.

14 ps arises from the onset of charge transfer. The PB signal probed at 700 nm shows a relatively slow rise (14 ps) and long-lived character that is similar to the PIA signal shown in Figure 5b, again consistent with the charge-separated state.

### 3. Discussion

Both OTV and OTV:PCBM films exhibit photoexcitation dynamics different from that typically found in conjugated polymers (e.g., PPVs and PTs). The oligomer chains in OTV exhibit predominantly neutral photoexcitations with much shorter lifetimes, as is evident from the relaxation dynamics

displayed in Figures 3 and 4. We note that films made of shorter oligomers (2TV and 3TV) actually display much longer excitation times ( $\tau_{\text{exc}}$ ),<sup>[11]</sup> consistent with the larger HOMO–LUMO gap.

Following the usual assignment of the PIA bands in conjugated polymers (by Vardeny et al.<sup>[13–15]</sup>), we assign the PIA band at near IR (1000 nm) regime in OTV to intrachain excitons that decay with a time constant of 0.6 ps; the PIA band at the absorption edge around 750 nm, (which we find to rise with 300 fs and decay with 1.6 ps, as indicated in Fig. 4) has been assigned to interchain trapped polaron pairs.

The observed electron-transfer time in OTV:PCBM is 14 ps (as indicated in Fig. 5), i.e., significantly longer than the sin-

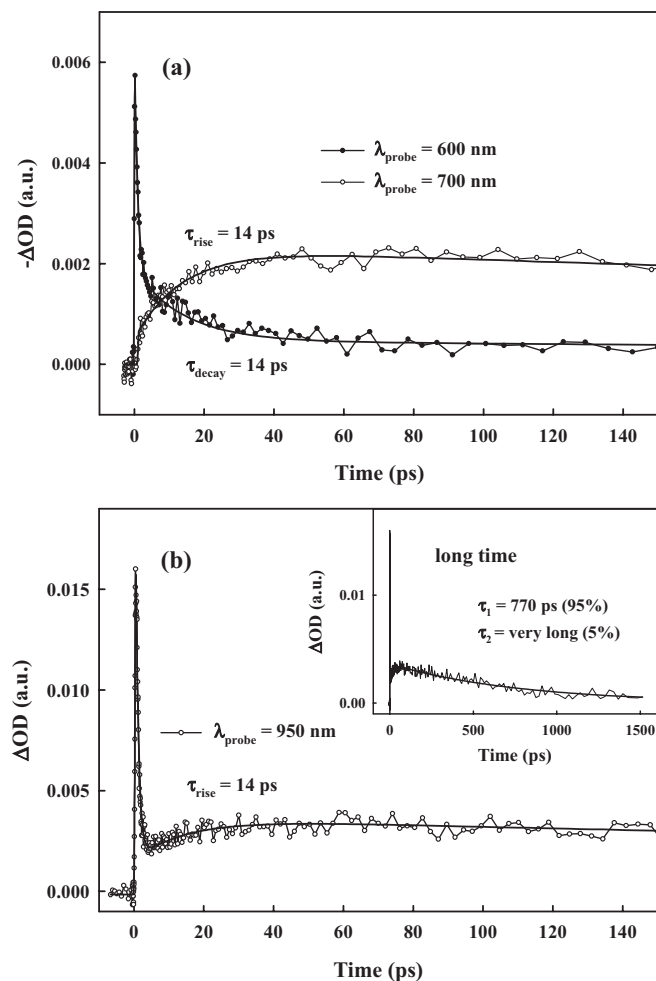


**Figure 5.** a,b) Transient absorption-decay profiles of OTV:PCBM (1:1) film in the long time regime. The decays were probed at 600 and 700 nm (a), and at 950 nm (b) using a time-window of 150 ps. The inset of (b) reveals the decay profile monitored with a longer time-window of 1500 ps. The pump wavelength used was 650 nm.

plet-state lifetime of 0.6 ps in OTV. Assuming that the efficiency of the charge-transfer process is proportional to the ratio of these two times, we conclude that the electron-transfer yield is less than 5% in the OTV:PCBM composite, much smaller than observed in conjugated polymer:C<sub>60</sub> composites. Once an electron is transferred onto the PCBM site, however, the lifetime of the charge-separated state is relatively long, as indicated from the data in Figures 2 and 5.

The reason for the exceptionally small electron-transfer yield in the OTV:PCBM composite compared to that observed in conjugated-polymer:C<sub>60</sub> composites is intriguing, in particular because the LUMO energy level in OTV lies significantly higher in energy than the LUMO energy level in PCBM (−3.2 eV<sup>[16]</sup> and −4.2 eV, respectively). One plausible explanation for this behavior is based on the Rice model<sup>[17]</sup> of charge transfer in semiconducting polymers, where the π- and π\*-bands form a continuum of energy levels. According to the Rice model, upon photoexcitation of an electron from the π- to the π\*-band, as the electron is transferred to the lower level

(i.e., from the LUMO in the donor to the LUMO in the acceptor) the requirement of energy conservation for the entire process leads to the excitation of the geminate hole (via the electron-hole Coulomb interaction). The excited hole absorbs the energy difference between the donor and acceptor LUMO levels. Because of the rapid energy conservation, enabled by excitation of the hole in the continuum of the π-band, there is no “bottleneck”, and the electron-transfer reaction is therefore ultrafast. In oligomers, however, the discrete nature of the electronic levels will generally limit the hole to a discrete set of energy levels. If energy conservation is therefore not directly allowed, a bottleneck is created. Because the discrete electronic levels vary in time because of lattice vibrations, an exact energy match can be obtained after a time span on the order of the lattice vibration period, thereby relieving the bottleneck. Thus, for very general reasons we expect the electron-transfer rate to be slower in conjugated oligomers than in conjugated polymers. We note that other mechanisms may also play a role in the long charge-transfer time observed in OTV:PCBM. For example, the large energy difference between the LUMO of the donor and the LUMO of the acceptor (approximately 1 eV) will likely put the system in an inverted Marcus regime.<sup>[18]</sup> In addition, the exciton-binding energy in oligomers is typically larger than in the corresponding polymers. A larger exciton-binding energy will also inhibit electron transfer.

Finally, we comment on the coherent oscillations that are clearly seen in the PB signal probed at 700 nm in OTV. A plausible origin for these oscillations in the PB signal is the generation and propagation of acoustic sound waves across the OTV film. As described by Thomsen et al., the laser pulse creates a plane of stress that initiates a longitudinal acoustic wave that propagates back and forth across the film.<sup>[19,20]</sup> The accompanying strain induced by this sound wave modifies the electronic levels in the semiconductor (e.g., the HOMO–LUMO energy gap), and thereby modulates the absorption and/or bleaching time-delayed signals.<sup>[19,20]</sup> Such a stress wave is typically generated as a result of the excess photon energy (i.e., the difference between the pump photon energy and the absorption edge); however, because of the nonradiative fast (0.6 ps) decay of the singlet-state in OTV, a higher portion of the pump energy contributes to the photoinduced change in the surface temperature that launches the acoustic sound wave. Using the measured period in OTV, τ<sub>0</sub> = 310 ps, and the relation τ<sub>0</sub> = 4d/v<sub>s</sub>,<sup>[19]</sup> where *d* is the film thickness (ca. 120 nm in case of Fig. 4) and v<sub>s</sub> the sound velocity, we find that in OTV v<sub>s</sub> = 1.6 × 10<sup>5</sup> cm s<sup>−1</sup>; a value which is reasonable for an organic material and comparable to the value 2.5 × 10<sup>5</sup> cm s<sup>−1</sup> determined in the same way in As<sub>2</sub>Te<sub>3</sub>.<sup>[19]</sup> Experiments conducted on few OTV samples with different film thicknesses, described in the Supporting Information, revealed that the period is linearly proportional to the film thickness *d*, as expected from the above equation for τ<sub>0</sub>.

## 4. Conclusions

We describe the photoexcitation relaxation dynamics in oligo(thienyleneviylene) (OTV) and in an OTV:C<sub>60</sub> composite.

We find that in the OTV:PCBM composite, the photoexcitations decay primarily through intrachain relaxation rather than intermolecular electron transfer. The rate of the photoinduced electron transfer process in OTV:PCBM is approximately  $7 \times 10^{10} \text{ s}^{-1}$  (14 ps). Because the singlet-state relaxation rate in OTV is  $1.7 \times 10^{12} \text{ s}^{-1}$  (0.6 ps), the deduced quantum efficiency for photoinduced electron transfer is less than 5%. When probed at 700 nm, we detect a coherent modulation of the photobleaching signal in OTV, a behavior indicative of the generation and propagation of acoustic sound waves in the OTV film. From the period of these modulations we deduced a sound velocity of  $1.6 \times 10^5 \text{ cm s}^{-1}$  in OTV.

## 5. Experimental

The OTV, with ten repeat units (shown in Scheme 1), was prepared as described previously [21]. The  $C_{60}$  derivative, PCBM, was provided by Konarka Technologies. In order to study the electron-transfer dynamics in the high concentration regime relevant to photovoltaic cells, OTV:PCBM composites containing 50% (w/w) PCBM were prepared. All films (both pristine OTV and blended OTV:PCBM) were spin-cast from chlorobenzene solution ( $10 \text{ mg mL}^{-1}$ ) onto quartz substrates. The films had an optical density approximately equal to 1.0 at the maximum absorption. Following spin-casting, the films were baked for 1 h at  $60^\circ\text{C}$  to remove any residual solvent. The samples were loaded into a vacuum chamber in a dry glove-box filled with nitrogen and kept under a dynamic vacuum ( $< 10^{-4}$  mbar) during measurements.

The dual-beam femtosecond spectrometer that was employed for the transient absorption (TA) measurements consisted of the second harmonic of OPA (optical parametric amplification) pump and a white-light continuum probe [22]. The TA spectra were determined by probing the TA decay at each wavelength using constant pump fluence. At each probe energy, the various decay time constants were obtained after first de-convoluting the measured signal with respect to the pump Gaussian time-profile (characterized by a full width at half maximum of 120 fs) and then fitting the signal decay to exponential terms.

Transient photoconductivity measurements were carried out in the Auston switch configuration using the 120 fs laser pulses tuned at 400 nm (the 2nd harmonic generation of the regenerative amplifier output) and a boxcar integration system, with an overall time resolution of approximately 100 ps. The pristine OTV and blended OTV:PCBM films were spin-cast onto alumina ( $\text{Al}_2\text{O}_3$ ) substrates on which planar Au contacts with a gap between the electrodes of  $150 \mu\text{m}$  were evaporated to form the photoconductive switch. The laser excitation beam diameter was approximately  $500 \mu\text{m}$ .

Received: March 23, 2006

Revised: May 2, 2006

Published online: January 26, 2007

- [1] N. S. Sariciftci, L. Smilowitz, A. J. Heeger, F. Wudl, *Science* **1992**, 258, 1474.
- [2] B. Kraabel, C. H. Lee, D. McBranch, D. Moses, N. S. Sariciftci, A. J. Heeger, *Chem. Phys. Lett.* **1993**, 213, 389.
- [3] B. Kraabel, D. McBranch, N. S. Sariciftci, D. Moses, A. J. Heeger, *Phys. Rev. B: Condens. Matter Mater. Phys.* **1994**, 50, 18543.
- [4] C. J. Brabec, G. Zerza, G. Cerullo, S. D. Silvestri, S. Luzzati, J. C. Hummelen, S. Sariciftci, *Chem. Phys. Lett.* **2001**, 340, 232.
- [5] P. A. van Hal, R. A. J. Janssen, G. Lanzani, G. Cerullo, M. Zavelani-Rossi, S. D. Silvestri, *Chem. Phys. Lett.* **2001**, 345, 33.
- [6] W. Ma, C. Yang, X. Gong, K. Lee, A. J. Heeger, *Adv. Funct. Mater.* **2005**, 15, 1617.
- [7] J. Y. Kim, S. H. Kim, H.-H. Lee, K. Lee, W. Ma, X. Gong, A. J. Heeger, *Adv. Mater.* **2006**, 18, 572.
- [8] H. Fuchigami, A. Tsumura, H. Koezuka, *Appl. Phys. Lett.* **1993**, 63, 1372.
- [9] A. P. Smith, R. R. Smith, B. E. Taylor, M. F. Durstock, *Chem. Mater.* **2004**, 16, 4687.
- [10] S. D. Halle, M. Yoshizawa, H. Murata, T. Tsutsui, S. Saito, T. Kobayashi, *Synth. Met.* **1992**, 49–50, 429.
- [11] J. J. Apperloo, C. Martineau, P. A. van Hal, J. Roncali, R. A. J. Janssen, *J. Phys. Chem. A* **2002**, 106, 21.
- [12] M. Fujitsuka, A. Masuhara, H. Kasai, H. Oikawa, H. Nakanishi, O. Ito, T. Yamashiro, Y. Aso, T. Otsubo, *J. Phys. Chem. B* **2001**, 105, 9930.
- [13] R. Österbacka, C. P. An, X. M. Jiang, Z. V. Vardeny, *Science* **2000**, 287, 839.
- [14] X. Jiang, R. Österbacka, O. Korovyanko, C. P. An, B. Horovitz, R. A. J. Janssen, Z. V. Vardeny, *Adv. Funct. Mater.* **2002**, 12, 587.
- [15] S. V. Frolov, M. Liess, P. A. Lane, W. Gellermann, Z. V. Vardeny, M. Ozaki, K. Yoshino, *Phys. Rev. Lett.* **1997**, 78, 4285.
- [16] A. Henckens, K. Collandret, S. Fourier, T. J. Cleij, L. Lutsen, J. Gelan, D. Vanderzande, *Macromolecules* **2005**, 38, 19.
- [17] M. J. Rice, Y. N. Gartstein, *Phys. Rev. B: Condens. Matter Mater. Phys.* **1996**, 53, 10764.
- [18] R. A. Marcus, *Angew. Chem. Int. Ed. Engl.* **1993**, 32, 1111.
- [19] C. Thomsen, J. Strait, Z. Vardeny, H. J. Maris, J. Tauc, J. J. Hauser, *Phys. Rev. Lett.* **1984**, 53, 989.
- [20] D. Lim, R. D. Averitt, J. Demsar, A. J. Taylor, N. Hur, S. W. Cheong, *Appl. Phys. Lett.* **2003**, 83, 4800.
- [21] I. Jestin, P. Frère, N. Mercier, E. Levillain, D. Stievenard, J. Roncali, *J. Am. Chem. Soc.* **1998**, 120, 8150.
- [22] D. Moses, A. Dogariu, A. J. Heeger, *Phys. Rev. B: Condens. Matter Mater. Phys.* **2000**, 61, 9373.